18th Australasian Fluid Mechanics Conference
Launceston, Australia
3-7 December 2012

Three dimensional conditional structure of large-scale structures in a high Reynolds number turbulent boundary layer

K. M. Talluru[1], C. Morrill-Winter[2], R. Ebner[2], N. Hutchins[1], J. Klewicki[1,2], and I. Marusic[1]

[1]Department of Mechanical Engineering
The University of Melbourne, Victoria, 3010 AUSTRALIA

[2]Mechanical Engineering Department
The University of New Hampshire, New Hampshire, 03824 USA

Abstract

A novel configuration of using a multiple hot-wire probe and an array of skin-friction sensors is developed to study the three dimensional conditional organization of large scale structures in a high Reynolds number turbulent boundary layer. The current study is an extension of the previous work carried out by Hutchins *et al.* [6] in analyzing the conditional average maps and the amplitude modulation of small scale fluctuations. However, we here report results based on all three components of velocity. The results are significant in two distinct ways, providing deeper insights to the dynamics of the large-scale structures; (1) They show that small-scale v, w and $\langle -uw \rangle$ are modulated in a very similar manner to that of u, and (2) They demonstrate the existence of roll-modes associated with superstructure events. These have not previously been shown for laboratory data at high Reynolds numbers.

Introduction

In the past few decades, there has been significant research towards understanding large scale coherence in turbulent boundary layers, especially in high Reynolds number flows. The origin of this dates back to the findings of Blackwelder and Kovasznay [1], who observed elongated regions of uniform streamwise momentum from the streamwise velocity fluctuations. Over the last decade, numerous studies using techniques such as hot-wire anemometry, Direct Numerical Simulations(DNS) and Particle Image Velocimetry(PIV), have substantiated the spatial and temporal nature of these large structures. PIV studies by Tomkins and Adrian [9] have revealed the spatial nature of these structures in the instantaneous fields of streamwise velocity. Hutchins and Marusic [3] used a rake of hot wires and from the time series data, they reported that these structures extend to large streamwise lengths and substantially meander in the spanwise direction. In addition, they also identified that these large scale structures maintain a footprint at the wall.

This was explored by Hutchins *et al.* [6], who used the large-scale shear-stress foot-print at the wall to obtain a three dimensional conditionally averaged view of the large-scale superstructures in a turbulent boundary layer, also investigating how these features modulate with the small-scale fluctuations near the wall. Their study, however, solely employed measurements of streamwise velocity which limited their characterization of the large-scale modulating events. Several studies have also investigated the wider spanwise organization of the very large-scale structures. Hutchins and Marusic [4] identified counter rotating roll-like structures associated with the largest scale events using a DNS channel flow database ($Re_\tau = 950$). From high speed PIV measurements, Dennis and Nickels [2] computed various conditional averages and showed a similar organization in the spanwise vicinity of large-scale structures. Such a phenomenon was also observed by Hutchins *et al.* [5] in their atmospheric boundary layer studies. They reported such features not just in the conditional average maps but also in the instantaneous velocity vector fields in the spanwise wall-normal planes. We here extend the current understanding of these superstructures by measuring all the three velocity components associated with these events. Such analysis provides a more detailed picture of the large-scale motions and their interactions with the near wall turbulent motions.

Experimental setup

Experiments are carried out in the high Reynolds number boundary layer wind tunnel (HRNBLWT) at the University of Melbourne, full details of the wind tunnel are given in [7]. Measurements were taken at a streamwise distance of 23 m from the trip. The free stream velocity is set at 10 m/s, with a nominal boundary layer thickness of 0.3 m and friction velocity, $U_\tau = 0.335$ m/s giving a friction Reynolds number $Re_\tau \approx 7000$ ($Re_\tau = U_\tau \delta/\nu$, where U_τ is the friction velocity, δ is the boundary layer thickness and ν is the kinematic viscosity). The experimental setup is shown in figure 1. It consists of 9 flush-mounted skin friction sensors arranged in a spanwise array along with a multiple hot wire probe fixed to a movable traverse and positioned right above the middle shear-stress sensor of the spanwise array. The wall shear stress sensors are Dantec 55R47 glue on type and are operated in constant temperature mode with a overheat ratio (OHR) of 1.05 using an AA labs AN 1003 anemometer, while the hot-wires are operated with a OHR of 1.5 using in-house developed Melbourne University Constant Temperature Anemometer (MUCTA). The dimensions, specifications and relative positions of the skin-friction sensors are similar to the configuration used by Hutchins *et al.* [6]. Throughout this paper, x, y, z refer to the streamwise, spanwise and wall-normal directions while u, v, w represent the corresponding fluctuating velocity components.

The multiple hot-wire probe, here onwards referred to as the 'uvw' probe, consists of two single inclined wires and a conventional cross wire, as shown in figure 1. The two single wires (marked as 1 and 4) are inclined to the direction of flow and are positioned in the streamwise-spanwise plane to measure the u and v components, while the cross wire (2 and 3 together) yields the u and w components. All these wires are made of platinum-rhodium alloy, have a diameter ($d = 2.5\mu$m) and length ($l = 0.44$mm) and are welded to the tips of custom-built prongs. More details of the design of 'uvw' probe are given in [10]. The hot wires are calibrated using a computer controlled round jet which is pitched and yawed about the axis of the probe at multiple angles and at different velocities to produce a 3D calibration surface. The hot-film sensors are calibrated using the friction velocity values obtained from previously reported results at the same location. Any errors in hot-film calibration will have only minimal effect on the analysis presented here since these sensors are merely used as low/high skin-friction

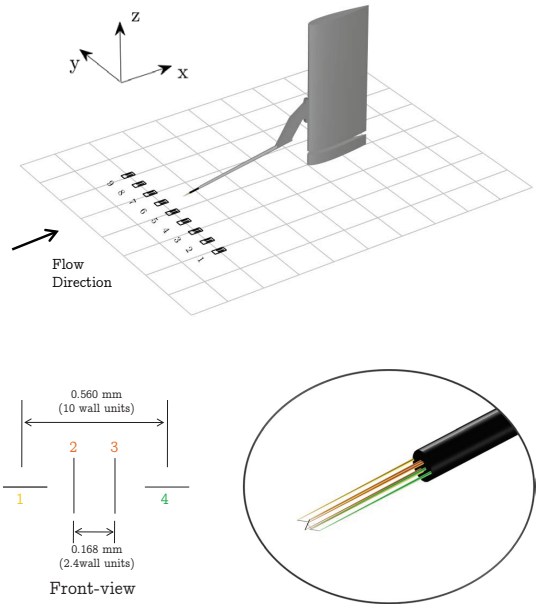

Figure 1: Schematic of Multiple hot-wire setup

detection sensors.

Three dimensional conditional view

The three dimensional structure of the superstructures can be studied by computing various quantities from the 'uvw' probe conditioned on the passage of a low or high skin friction event. The signal from the wall shear stress sensor is used to detect the structures convecting above it. This signal is filtered using a gaussian filter of length 0.5δ to get the pure signature of a large-scale event and eliminate small-scale energy. From this large-scale signal, a low skin-friction event is identified when its value is below zero and conversely, a value above zero indicates a high skin-friction event. The traversing hot-wire signal is conditionally sampled on the occurrence of a low or high friction event at each of the 9 spanwise skin-friction sensors, enabling us to build a volumetric view of the conditionally averaged velocity fluctuations associated with this event $\tilde{u}|_l$.

$$\tilde{u}|_l(\Delta t,\Delta y,z) = \langle u(t,y,z) \mid u_\tau(t-\Delta t, y-\Delta y) < 0 \rangle \qquad (1)$$

Here u can be any of the three normalized-velocity fluctuations and u_τ is the fluctuating friction velocity signal. The hot-wire and shear-stress signals are time-series signals but by applying Taylor's hypothesis ($x = -U_c t$), we can convert to spatial coordinates. U_c here is the convection velocity of the large-scale events taken to be $U_c = 7$ m/s (the velocity at the midpoint of the log-region as suggested in Hutchins *et al.* [6].

$$\tilde{u}|_l(\Delta x,\Delta y,z) = \langle u(x,y,z) \mid u_\tau(x-\Delta x, y-\Delta y) < 0 \rangle. \qquad (2)$$

As shown by equations 1 and 2, it is possible to generate a volumetric view of the conditional structure by varying Δt, Δy and z, all of which are possible with our experimental setup. The simultaneous time series signals from the spanwise array and wall normal traversing sensor enable us to compute these conditional quantities. To maintain the uniformity of results across the paper and to draw a direct comparison with previously reported results, only the low skin-friction conditioned events are shown here. These are nominally the negative of the high skin-friction conditional averages.

Velocity fluctuations

Using the 'uvw' probe, fluctuating signals of all three components of velocity were obtained and the conditional averages of fluctuations were computed. The iso-contours of $\tilde{u}|_l^+$, $\tilde{v}|_l^+$ and $\tilde{w}|_l^+$ are shown in figures 2, 3 and 4 respectively, in different planes chosen to show the three dimensional nature of a characteristic low-speed event centered at $\Delta x = \Delta y = z \approx 0$. In each of these figures,the $x-y$ plane is drawn at a location $z/\delta \approx 0.002$, the $x-z$ plane is shown at $\Delta y = 0$ (the centreline of the detected large-scale event) and five streamwise slices in the $y-z$ plane are displayed at locations $\Delta x/\delta = -2,-1,0,1,2$. Note that a linear scale is used for the z direction.

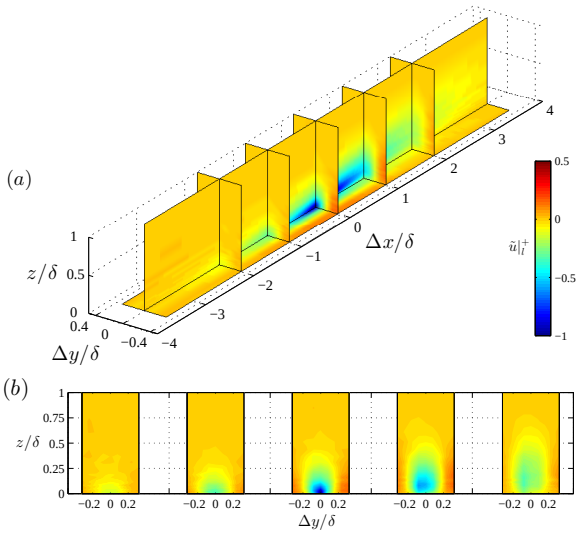

Figure 2: Iso-contours of u^+ velocity fluctuations conditionally averaged on a low skin-friction event

Figure 2(a) shows an elongated forward-leaning large low-speed feature, extending to a distance of 5δ in streamwise direction. This result is totally consistent with the recent study of Hutchins *et al.* [6]. The spanwise distribution is more clearly seen in figure 2(b), with the low-speed region flanked by high speed regions on either sides. The width of the low-speed region appears to be 0.5δ in the plane at $\Delta x = 0$. It is also clear that there is streamwise growth of the conditional structure, with the strong negatively correlated region moving away from the wall as we move downstream of the conditioning point.

Figure 3 shows the conditional view of v fluctuations. A nominally zero fluctuation region is observed across the entire center line plane ($\Delta y = 0$) with elongated regions of opposite correlations on either side of it. Such regions are extending to a distance of 2δ in the streamwise direction. Close to the wall, this shows that the large-scale low friction event is accompanied by spanwise converging motion. Further from the surface this switches to diverging motion. As will be elaborated on below, such patterns are consistent with large-scale roll-modes accompanying the superstructure events. The extent of correlations is better understood in figure 3(b). It appears that there are opposite correlations of equal strength about the plane $\Delta y = 0$ separated approximately by 0.5δ.

The conditional average map of wall-normal fluctuations is shown in figure 4. Comparing figures 2 and 4 reveals a strong anti-correlation between u and w events. The large-scale forward leaning low-speed events (that accompanies the negative u_τ fluctuation at the wall) is also characterized by a large-scale region of positive w (flow away from the wall). Thus low-speed fluid is ejected away from the surface on the centreline of these large-scale events. Flanking this region, we note that the high-

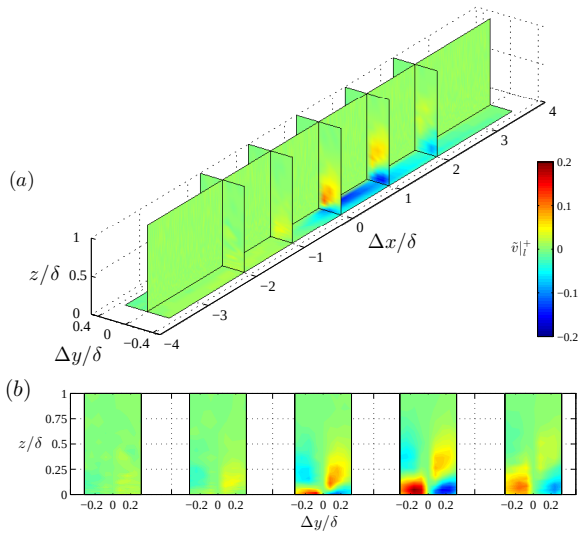

Figure 3: Iso-contours of v^+ velocity fluctuations conditionally averaged on a low skin-friction event

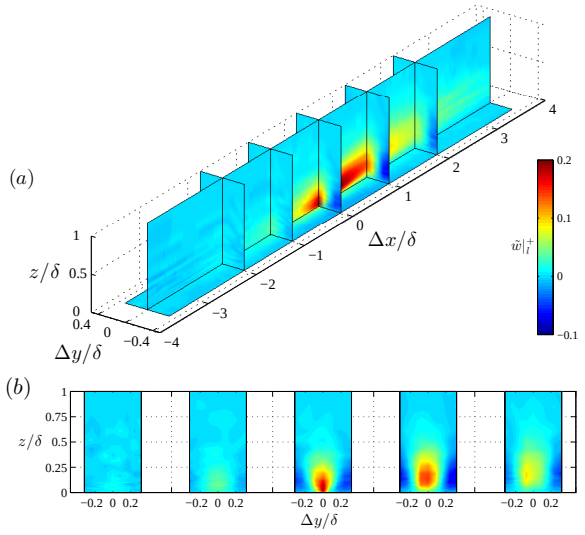

Figure 4: Iso-contours of w^+ velocity fluctuations conditionally averaged on a low skin-friction event

speed positive u fluctuations from figure 2 are accompanied by negative w (sweeping of high-speed fluid towards the surface).

A closer analysis of the directions of v and w fluctuations in the conditional plots of figures 3 and 4 reveals the existence of large-scale roll modes. This is best illustrated by plotting the $v-w$ vector field in the planes $\Delta x/\delta$ = 0, 1 and 2, as shown in figure 5. The observed counter-rotating roll modes are very large, extending to a width of 0.3δ and extending to a height of 0.4δ. A comparison of the core of these roll modes (marked by the symbol $\oplus$) at different Δx planes reveals that they are inclined to the wall with a characteristic angle of approximately 9^o.

Amplitude modulation of small scale energy

The phenomenon of large scale structures modulating the amplitude of the small scale energy has been studied by Hutchins and Marusic [4] and has been the basis of a successful prediction model by Marusic *et al.* [8]. A volumetric conditionally averaged view of the small-scale energy in u based on the occurrence of a large-scale low skin-friction event has been shown by

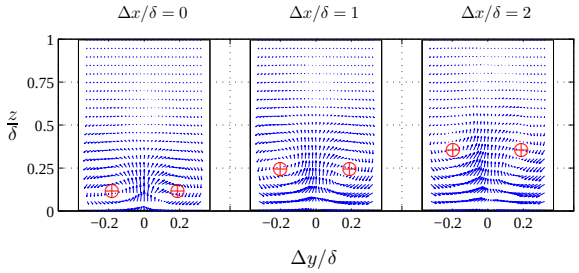

Figure 5: Roll-modes, observed in the planes $\Delta x/\delta = 0$, 1 and 2

Hutchins *et al.* [6]. We here extend this view to include small-scale v and w fluctuations. To carry out such an analysis, the signals from the hot-wire probe are filtered using a spectral cut-off filter at $\lambda_x^+ = 7000$, to leave only the small-scale components $\lambda_x^+ < 7000$. Such a filter was previously shown by Hutchins and Marusic [4] to effectively separate the inner and outer peaks in the energy spectra of u fluctuations, although it is not entirely clear that it will be as effective for v and w fluctuations. The conditional scheme is similar to the earlier detections, only in this case we ensemble average the change in small-scale variance:

$$\tilde{u_s^2}|_l(\Delta x,\Delta y,z) = \langle u_s^2(x,y,z) \mid u_\tau(x-\Delta x, y-\Delta y) < 0\rangle - \overline{u_s^2} \quad (3)$$

Here, u_s is the small scale signal and the $u_s^2|_l$ is the conditionally averaged small-scale fluctuations associated with large-scale low skin-friction event ($u_\tau < 0$). Note that $u_s^2|_l$ is the conditionally averaged small scale variance as compared to the unconditional small-scale variance $\overline{u_s^2}$.

The three dimensional view of conditional averages of small-scale variance of u, v and w components based on the occurrence of a low skin-friction event is shown in figure 6. The color scale used in this plot is an indication of percentage change in conditioned small-scale variance about the time-averaged unconditional small-scale variance. The amplification of small-scale energy is shown in red shading while the blue shows attenuation. Note that a logarithmic scale is used for the z direction.

In all these results, we observe that small scale energy is attenuated near the wall and amplified farther away from the wall within a low skin-friction event. Conversely, an opposite phenomenon is observed when conditioned on the passage of a large-scale high-speed event. These results are entirely consistent with those shown by Hutchins *et al.* [6]. The change over from attenuation to amplification seems to occur at increasing distances from the wall as we move downstream from $\Delta x/\delta = -\delta$ to 2δ. A similar trend is noticed in the conditional average plot of Reynolds shear stress shown in figure 7 which is computed using a conditional scheme similar to the one previously explained in equation 1. The implications of these results are many, two of which are highlighted here. It suggests a possibility to extend the recently developed prediction model of Marusic *et al.* [8] to include other components of velocity. In addition, since the large-scale superstructure events clearly modulate the near-wall cycle, it might suggest control schemes targeting large-scale structures could be a viable avenue of future research.

Conclusions

With the use of a multiple traversing hot-wire probe and flush-mounted array of skin friction sensors, simultaneous measurements of all three velocity components were obtained and analysis of various conditional averages and conditional variance was carried out. The conditional mean results illustrate the presence of very long, forward-leaning low/high speed struc-

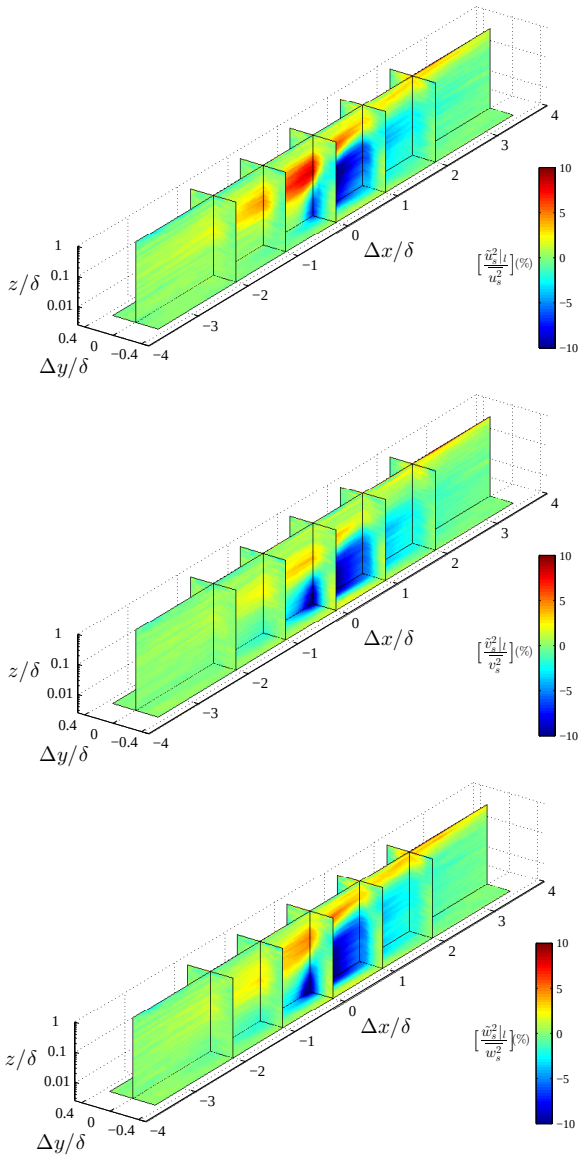

Figure 6: Iso-contours of percentage change in the small scale variance of the three velocity components conditionally averaged on a low skin-friction event

tures in the streamwise direction, flanked by high/low speed regions, respectively. Such a low/high speed large-scale event is also characterized correspondingly by a large scale positive/negative fluctuations in w. A closer look at the conditional average maps of v and w fluctuations show the presence of large counter-rotating roll-modes that extend over 2δ streamwise lengths. This three dimensional conditional structure of a low-speed event, is found to be consistent with those reported previously by Dennis and Nickels [2] and also in the recent findings of Hutchins *et al.* [5] in their atmospheric boundary layer studies. From the conditional variance results, it is observed that the low-speed structure associated with negative u_τ fluctuation at the wall, consists of reduced small-scale activity near the wall switching to a region of intense small-scale fluctuations farther away from the wall. This phenomenon is observed universally in the small-scale variance of u, v and w components and the Reynolds shear-stress $\langle -uw \rangle$, suggesting that the prediction model of Marusic *et al.* [8] could be extended to other components of velocity. In conclusion, the results strongly confirm the finding that small-scale structures near the wall are influenced by the passage of large-scale events in the outer layer.

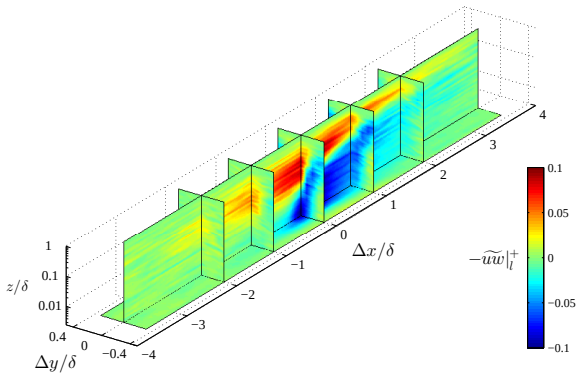

Figure 7: Iso-contours of Reynolds shear-stress fluctuations conditionally averaged on a low skin-friction event

Acknowledgements

The authors gratefully acknowledge support from the Australian Research Council.

References

[1] Blackwelder, R. F. and Kovasznay, L. S. G., Time scales and correlations in a turbulent boundary layer. Phys. Fluids 15, 1545-1554, 1972

[2] Dennis, D. J. C. and Nickels, T. B., Experimental measurement of large-scale three-dimensional structures in a turbulent boundary layer. Part 1. Vortex packets, *J. Fluid Mech.*, 673:180-217, 2011.

[3] Hutchins, N. and Marusic, I., Evidence of very long meandering structures in the logarthimic region of turbulent boundary layers. *J. Fluid Mech.*, 579:1-28, 2007a.

[4] Hutchins, N. and Marusic, I., Large-scale influences in near-wall turbulence. *Phil. Trans. R. Soc. A*, **365**, 2007b, 647-664.

[5] Hutchins, N. and Chauhan, K. and Marusic, I. and Monty, J. and Klewicki, J., Towards Reconciling the Large-Scale Structure of Turbulent Boundary Layers in the Atmosphere and Laboratory, Boundary-Layer Meteorology, 0006-8314, 1-34, 2012.

[6] Hutchins, N., Monty, J. P., Ganapathisubramani, B., H. C. H. Ng., and Marusic, I., Three-dimensional conditional structure of a high-Reynolds-number turbulent boundary layer. *J. Fluid Mech.*, 673:255-285, 2011.

[7] Kulandaivelu, V. Evolution of zero pressure gradient turbulent boundary layers from different initial conditions, PhD Thesis, The University of Melbourne, 2012.

[8] Marusic, I., Mathis, R. and Hutchins, N. Predictive Model for Wall-Bounded Turbulent Flow *Science.*, 329(5988), 193-196, 2010.

[9] Tomkins, C. D. and Adrian, R. J., Spanwise structure and scale growth in turbulent boundary layers. *J. Fluid Mech.*, 490:37-74, 2003.

[10] Vukoslavcevic, P. V., A hot-wire probe configuration and data reduction method to minimize velocity gradient errors for simultaneous measurement of three velocity components in turbulent flow. *Exp. Fluids*, Volume 53, 481-488, 2012.